

High Specific Contact Resistance of Ohmic Contacts to n-Ge Source/Drain and Low Transport Characteristics of Ge nMOSFETs

J. Oh¹, J. Huang¹, Y-T. Chen², I. Ok¹, K. Jeon³, S.-H. Lee²,
B. Sassman¹, W.-Y. Loh¹, H.-D. Lee⁴, D.-H. Ko⁵, P. D. Kirsch¹, and R. Jammy¹

¹SEMATECH, 2706 Montopolis Drive, Austin, TX 78741, USA

²Univ. of Texas, Austin, TX, ³Univ. of California, Berkeley, CA, ⁴Chungnam Nat'l. Univ., Korea, ⁵Yonsei Univ., Korea

Abstract

We address the low drive current issue with Ge nMOSFETs by analyzing source/drain (S/D) Ohmic metal contacts to n-type Ge using the transmission line method (TLM). Ni contacts to Ge nMOSFETs exhibit specific contact resistances of 10^{-3} ~ 10^{-5} Ω -cm², which is significantly higher than the 10^{-7} ~ 10^{-8} Ω -cm² of Ni contacts to Ge pMOSFETs. The high resistance of Ni Ohmic contacts to n-type Ge is attributed mainly to insufficient dopant activation in Ge (or high sheet resistance) and a high tunneling barrier. Results obtained in this work identify one of the root causes of the lower than expected Ge nMOSFET transport issue, advancing high mobility Ge channel CMOS technology.

Introduction

High mobility alternative channels have been researched to continue on the high performance roadmap where highly scaled Si channel CMOS has limitations. Ge and other high mobility channels potentially provide the high injection velocity to achieve projected high performance metrics. While the mobility enhancement for Ge pMOSFETs has been well reported [1-3], few studies have been able to improve Ge nMOSFET mobility after optimizing the gate stack and parasitic resistance [4-7]. Enhanced electron mobility of Ge nMOSFETs was demonstrated in long channel transistors, presumably to minimize the effects of high S/D parasitic resistance on transistor performance. In this work, we have quantitatively extracted specific contact resistance (ρ_c) of S/D Ohmic contacts to Ge and related them with Ge nMOSFET transport characteristics.

Device Fabrication

High quality epitaxial Ge channels are selectively grown on shallow trench isolation-formed Si substrates. A Si cap layer is deposited to improve the interface characteristics and off-state current. Hf-based gate oxide is atomic layer deposited followed by the metal gate. For the TLM test structure, the active region was defined, followed by S/D implantation and anneal. Then, deposited Ni metals were patterned on the TLM structure and rapid thermal annealed at 25~500°C.

Results and Discussion

Compared to Si pMOSFETs, Ge pMOSFETs enhance the drain current (Fig.1), transconductance (Fig.2), and mobility (Fig.3). However, Ge nMOSFETs tend to exhibit poor transport characteristics. Capacitance-voltage curves obtained for Si and Ge exhibit comparable accumulation capacitance for both n- and p-MOS capacitors (Fig.4). It is still debatable whether gate stack characteristics (i.e., interface trap density, D_{it}) is a primary cause of the Ge nMOSFET issue as enhanced hole mobility in Ge pMOSFETs is achieved with a relatively high D_{it} of the gate dielectric and Ge channels [8]. The relative performance of Si and Ge MOSFETs is in good agreement with total on-resistance (R_{total}) vs. gate length (L_g) results

(Fig.5,6). For nMOSFETs, R_{total} of the Ge channel is higher than the Si channel, resulting in low drain current in Ge nMOSFETs. For pMOSFETs, R_{total} of the Ge channel is lower than the Si channel and enhanced transport characteristics were obtained. Further analysis was made on S/D Ni Ohmic contacts to Ge and Si using TLM patterns (Fig.7,8). The specific contact resistance (ρ_c) and semiconductor sheet resistance (R_{sh}) were extracted from linear fits to the measured data using the extrapolated transfer length (L_t) and contact resistance (R_c) in equations $\rho_c = L_t^2 \cdot R_{sh}$ and $R_{sh} = R_c \cdot W / L_t$ [9]. Resistances were measured using the four-point probe technique. Measured R_c results of Ni contacts to Si and Ge for both n-type and p-type are shown at varying silicide or germanide formation temperatures in Fig.6. As-deposited (25°C) Ni contacts to n-type Ge (Fig.9) exhibit ρ_c (1.3×10^{-3} Ω -cm²), which is 3 orders of magnitude higher than Ni contacts to n-type Si (1.1×10^{-6} Ω -cm²). The ρ_c of the n-contact to Ge decreases with annealing. The lowest ρ_c of n-contacts to Ge is still higher than n-contacts to Si by more than 2 orders of magnitude, which degrades the transport characteristics of Ge nMOSFETs. Note that ρ_c of the p-contact to Ge at 25°C is 2.2×10^{-7} Ω -cm² (Fig.10). Further reduction in ρ_c of 2.7×10^{-8} Ω -cm² was obtained after annealing at 400°C. The overall ρ_c of p-contacts to Ge is lower than p-contacts to Si. The low ρ_c suggests a low electron barrier height (ϕ_B) of p-contacts to Ge due to Fermi-level pinning near the valence band edge for metal contacts to Ge and therefore high thermionic emission as $\rho_c \propto \exp[4\pi (\epsilon m^* / h)^{0.5} \cdot \phi_B / N_D^{0.5}]$. The doping concentration (N_D), which also determines the contact resistance and tunneling barrier, showed little difference in R_{sh} results (Fig.11) for p-Si and p-Ge. Note that R_{sh} of n-Ge is significantly higher than other semiconductors. Given an identical ion implantation into Si and Ge, high R_{sh} is caused by the low activation efficiency of Ge. A high R_{sh} increases parasitic resistances (i.e., contact and spreading resistances), resulting in poor transport in Ge nMOSFETs. The relatively higher electron ϕ_B than holes for metal contacts to Ge also contributes to the high ρ_c , which can be improved when combined with dopant activation, resulting in acceptable ρ_c for Ge n-contacts for potential highly scaled CMOS applications.

Conclusions

We have shown specific contact resistance results of Ni contacts to Si and Ge and their impact on n- and p-MOSFET performance. The lower drain current or mobility in Ge nMOSFETs is mainly caused by high parasitic S/D resistances, i.e., contact (ρ_c) and sheet (R_{sh}) resistances. TLM patterns exhibited 2~3 orders of magnitude high ρ_c for n-contacts to Ge because of insufficient n-type dopant activation, which compromises the transport characteristics of Ge nMOSFETs. For an alternative Ge channel CMOS approach, significant improvement in the n-contact to Ge is critical.

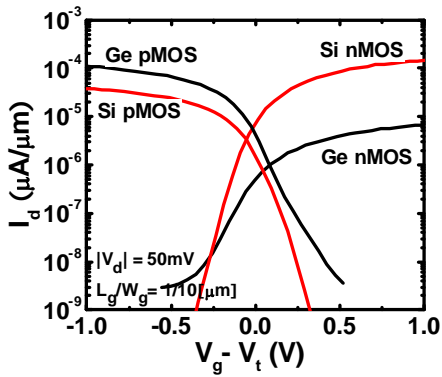


Fig. 1. I_D - V_G curves of Si and Ge CMOS. Enhanced drain current of Ge pMOSFETs. Low drain current of Ge nMOSFETs.

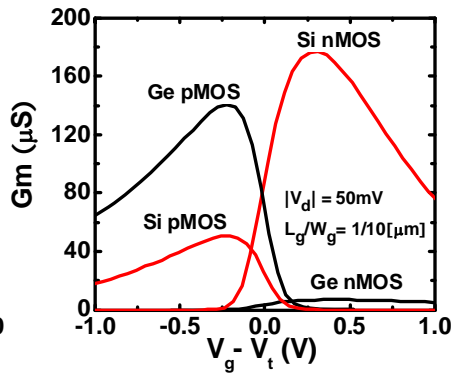


Fig. 2. Transconductance of Si and Ge CMOS. Enhanced G_m for Ge PMOSFETs, while degraded G_m for Ge nMOSFETs.

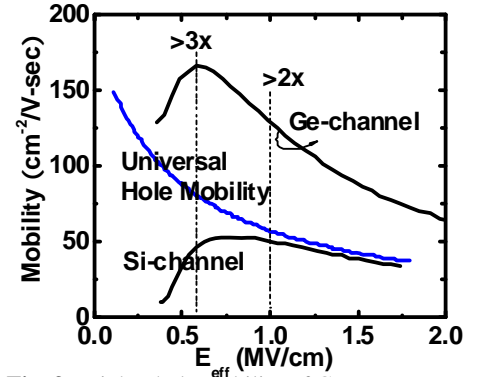


Fig. 3. Higher hole mobility of Ge pMOSFETs as compared to universal and reference Si pMOSFETs.

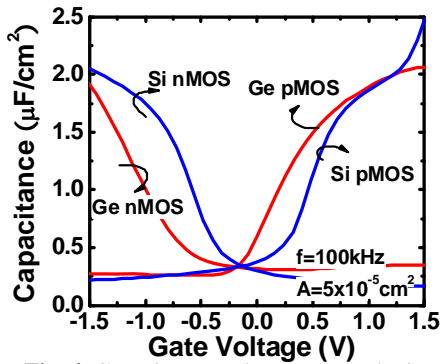


Fig. 4. Capacitance-voltage curves obtained for Si and Ge exhibit comparable accumulation capacitance for both n- and p-MOS capacitors

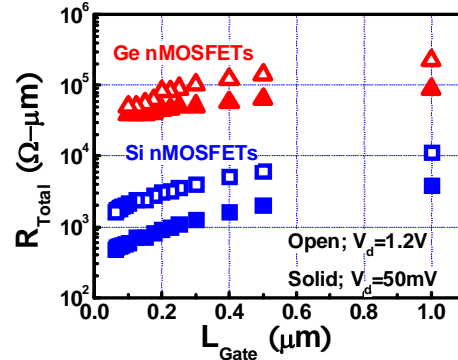


Fig. 5. Total on-resistance (R_{total}) vs. gate length. For nMOSFETs, R_{total} of the Ge channel is higher than the Si channel, resulting in low drain current in Ge nMOSFETs.

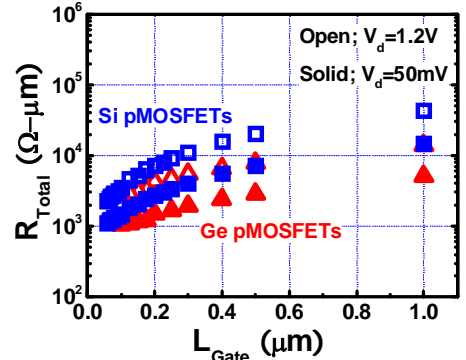


Fig. 6. For pMOSFETs, R_{total} of the Ge channel is lower than the Si channel and enhanced transport characteristics were obtained for Ge pMOSFETs.

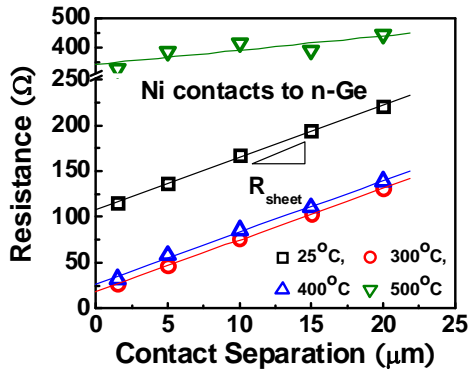


Fig. 7. ρ_c and R_{sh} are extracted from linear fits to the measured data. Contact resistance of Ni Ohmic contacts to p-Ge.

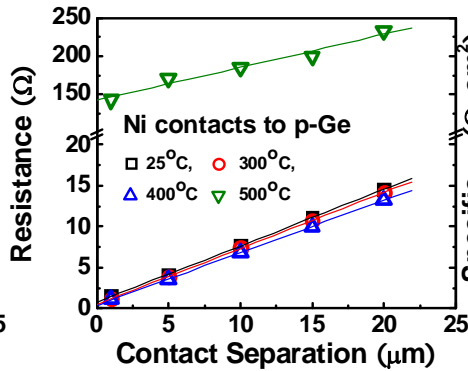


Fig. 8. Contact resistance of Ni Ohmic contacts to n-Ge. Equations $\rho_c = L_t^2 \cdot R_{sh}$ and $R_{sh} = R_c \cdot W/L_t$.

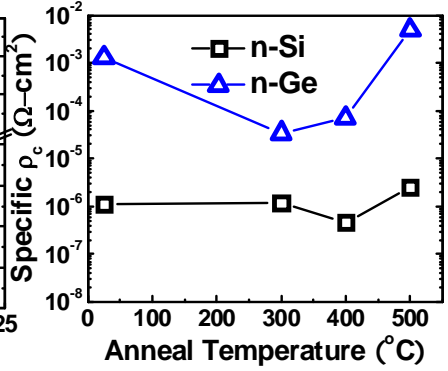


Fig. 9. Ni contacts to n-type Ge at 25°C exhibit higher ρ_c than Si, which degrades transport characteristics of Ge nMOSFETs.

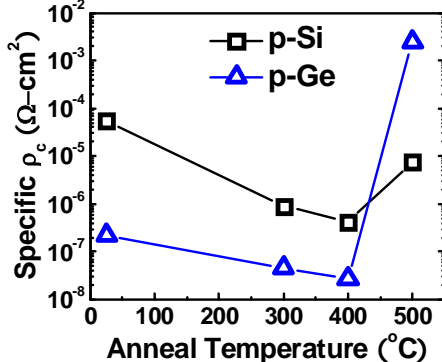


Fig. 10. ρ_c of p-contact to Ge at 25°C is $2.2 \times 10^{-7} \Omega\text{-cm}^2$. Further reduction in ρ_c of $2.7 \times 10^{-8} \Omega\text{-cm}^2$ is obtained at 400°C.

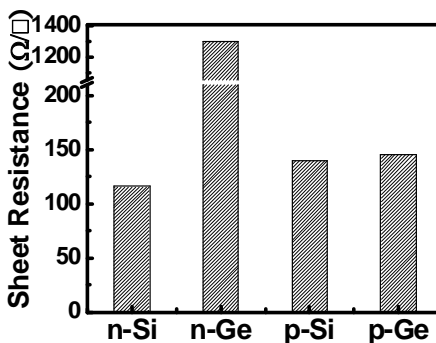


Fig. 11. Given identical ion implantation into Si and Ge, high R_{sh} of n-Ge is due to low dopant activation, degrading Ge nMOSFETs transport.

References

- [1] Y. Kamata 78 VLSI 2009.
- [2] N. Taoka 80 VLSI 2009
- [3] J. Mitard, VLSI 82 2009.
- [4] K. Morii, IEDM, 29.3, 2009.
- [5] D. Kuzum, IEDM, 19.1, 2009.
- [6] C.H. Lee, IEDM, 19.2, 2009.
- [7] M. Kobayashi, VLSI 76 2009.
- [8] J. Oh 238 VLSI 2009.
- [9] A. Crook, APL, 192114, 2007.
- [10] C. C. Han, J. Vac. Sci., Technol., B, p.1662, 1988.